Development of an ELISA to accurately measure the solubility of the amyloid beta 42 molecule

Elsa Ekström

LUND UNIVERSITY

LTH

FACULTY OF ENGINEERING

Department of Biochemistry and Structural Biology
Supervisor: Sara Linse
Assistant supervisors: Max Lindberg, Kalyani Sanagavarapu
Examiner: Kristine Steen Jensen

June 2024

Abstract

Amyloid beta (Aβ) proteins are a group of proteins able to form fibrillar aggregates that are linked to the adverse neurological effects seen in Alzheimer's disease [11]. The molecular mechanisms that lead to the Aβ aggregation are complex processes, and efforts to understand them are being made by investigating the kinetics and thermodynamic properties of the protein. The solubility of the protein is a central thermodynamic property governing the equilibrium between the non-aggregated forms and the aggregated forms [10]. To study the solubility, it is necessary to be able to study both aggregated and non-aggregated states. One method to study the non-aggregated state is with an enzyme-linked immunosorbent assay (ELISA).

The aim of this project was to develop an ELISA for the monomeric form of the Aβ42 peptide. The method was based on a previous ELISA described in Hellstrand et al. (2009) [8]. The goals of the method development was for the ELISA to be sensitive and to be selective for the Aβ42 monomer. With the method, an Aβ42 aggregation kinetics experiment described in Hellstrand et al. (2009) was reproduced. The method was developed for Aβ42 in a buffer environment, but the assay was also tested with Aβ42 in an environment of cerebrospinal fluid (CSF).

The method development was successful and the method showed satisfactory sensitivity and selectivity. Standard curves with linear regions between 1 and $\sim$30 nM Aβ42 were obtained. The limit of detection and limit of quantification of the method were shown to be in the low single-digit nanomolar range. The results from the aggregation kinetics experiment and the experiment described in the Hellstrand et al. (2009) paper varied slightly, possibly because of the ELISA being saturated or because of different fibril formations being achieved. The CSF experiments showed that unprocessed CSF has an interfering effect on the assay.

Acknowledgement

Firstly, I would like to thank Sara Linse for taking the role as my supervisor and enabling me to be involved in a fun and challenging project for my master thesis. I would like to give special thanks to my assistant supervisors Max Lindberg and Kalyani Sanagavarapu for answering many questions and guiding me through the interesting and complex field of amyloids and protein aggregation. Also, I would like to thank everyone in Sara Linses group for helping me with practical concerns in the lab. Lastly, I would like to thank Kristine Steen Jensen for taking the role as my examiner.

Contents

1 Introduction

Neurodegenerative diseases such as Alzheimer's disease (AD) have a serious negative effect on the health and the quality of life of those who suffer from them. It is estimated that 50 million people are affected by AD world wide, and the prevalence is expected to rise with an aging population [13]. While the exact cause behind the disease is unknown, years of research has given significant insights and there are currently a number of hypotheses that aim to explain the molecular mechanisms behind the disease [5]. One such hypothesis is the amyloid hypothesis. It suggests that the biological cause behind Alzheimer's disease is the misfolding and accumulation of a group of proteins referred to as amyloid β (Aβ) proteins [5]. It was proposed in the 1990's and is still the leading hypothesis [13]. Since the hypothesis was proposed, efforts have been made to develop methods that can be used to study the behaviour and characteristics of the Aβ proteins. The objective is that these methods can be applied in ways that improve clinical diagnosis, as well as enable research that will bring to light new understanding of the disease. This project aims to develop an enzyme-linked immunosorbent assay (ELISA) method for monomers of the Aβ42 protein, a type of Aβ protein. The method is intended to be a tool used used in research about Aβ42 solubility, and how the solubility is affected by different conditions and environments.

1.1 The Aβ peptide

Aβ proteins are products from the cleavage of the amyloid precursor protein (APP) [5]. APP is a transmembrane protein found in the central nervous system, and plays a role in several processes central for neurodevelopment, such as neuronal development, signaling, and intracellular transport, [4][5]. It undergoes cleavage with one of two pathways; the non-amyloidogenic, which happens in the majority of cases under physiological conditions, or the amyloidogenic pathway [4] . In the amyloidogenic pathway, APP gets cleaved into Aβ, a peptide chain with allomers ranging from 37 to 49 amino acids long [5]. The peptides have an N-terminus, (aa 1-16) and a hydrophibic C-terminus (aa 30 - to the end) [15]. A defining characteristic of amyloid proteins, including Aβ , is their ability to form insoluble aggregates [14]. These insoluble aggregates are referred to as fibrils and consist of a multimeric assembly of peptide in β-sheet formations [11], see **Figure 1.1**. Aβ is also able to form lower order assemblies, such as oligomers, which consist only of a few peptide molecules, and protofibrils [5]. The different assemblies are shown in **Figure 1.2**. It has previously been thought that it is the insoluble fibrils that cause the neurotoxicity of Aβ. However, now the belief has shifted towards soluble oligomeric forms being mainly responsible for the adverse affects of the peptide [5][13] .

The most readily produced Aβ variants are Aβ42 and Aβ40, peptides with 42 and 40 residues respectively [1]. In AD patients, the level of Aβ42 in cerebrospinal fluid (CSF) has been observed to decrease by 50% compared to normal levels [13]. The decrease in Aβ42 can be explained by the deposition of the peptide into insoluble

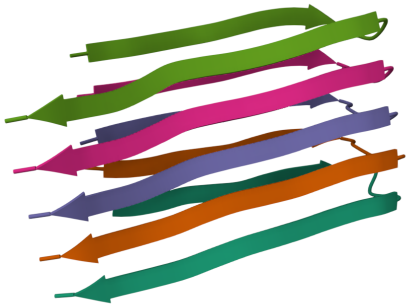

Figure 1.1: Structure of Aβ42 fibril. Retrieved from PDB file 2BEG.

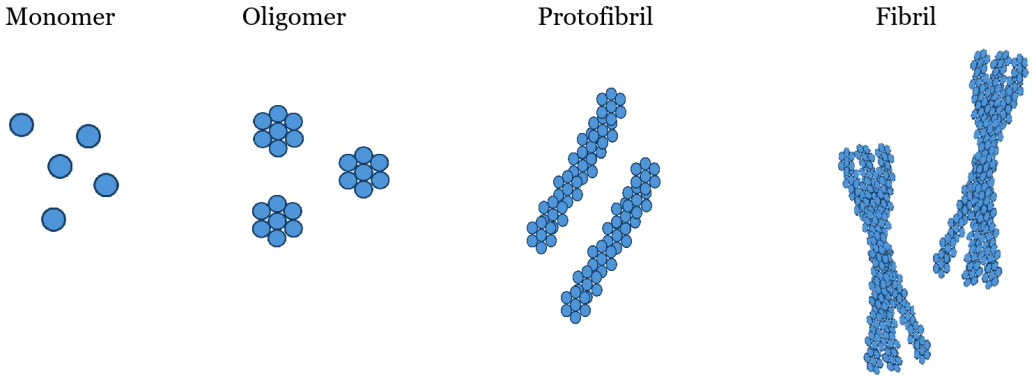

Figure 1.2: Schematic showing monomeric Aβ and its assemblies, in increasing order of complexity.

plaques in the brain [13]. Plaques are extracellular deposits of fibril bundles that have become entangled, and their presence in the brain has become a hallmark of AD [11] [5]. Another hallmark is the decrease in Aβ42, however the ratio of CSF Aβ42/Aβ40 is considered a better indicator of pathology [13].

1.2 Aggregation kinetics and solubility of the Aβ peptide

A central part of understanding Aβ peptides is understanding the mechanism by which they aggregate into fibrillar forms. Aggregation can be divided into three phases; lag phase, growth phase and a growth plateau, see **Figure 1.3**. The lag phase denotes the time period where aggregates are yet to be detected. The growth phase is the period where the rate of peptides assembling into aggregates is the greatest. The process by which peptides assemble into aggregates is made up of several microscopic processes that will not be discussed here, but it should be noted that their rate is dependent on the initial monomer concentration. Finally, the plateau is reached when the aggregate concentration, in a system of monomers and aggregates, has reached a stable value. In other words, the plateau is reached when monomer has reached its equilibrium concentration [2].

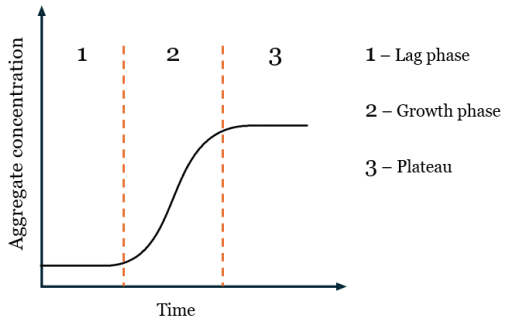

Figure 1.3: Schematic showing the different phases of aggregation expected, including the lag phase, growth phase and plateau.

The equilibrium concentration of monomer is a direct measure of the solubility of the peptide. The solubility can be described by a difference in standard chemical potential, see **Equation 1.1**. μ_m^0 denotes the standard chemical potential of the peptide as monomer in solution, and μ_f^0 the standard chemical potential of the peptide in fibrils. [10]

$$[m] = exp((\mu_f^0 - \mu_m^0)/RT) \tag{1.1}$$

In a paper by Hellstrand et al. (2009), Aβ fibril formation was investigated with kinetic aggregation experiments complemented by using ELISA to measure the monomer concentration [8]. For the kinetic aggregation experiments, thioflavin T (ThT) was used as a probe of the aggregation concentration [8]. ThT is a dye that binds only to the aggregated forms of Aβ, and not the monomer [10]. Thus, measured ThT fluorescence intensity is relative to the amount of aggregated Aβ [10]. **Figure 1.4 a)** shows the kinetic traces of the aggregation of three solutions of different intial Aβ42 monomer concentrations, published in Hellstrand et al. (2009). This graph illustrates how the rate of aggregation is concentration dependent. **Figure 1.4 b)** shows two graphs taken from the same paper. Here, they have taken Aβ42 samples that have been allowed to aggregate, isolated the monomer fraction of these samples (post-aggregation), and analysed the monomer fraction in an ELISA. This enabled them to plot the initial monomer concentration (total Aβ concentration) against the monomer concentration of the monomers that were left after aggregation (free Aβ concentration). The inital linear relationship between free and total Aβ, seen in b), can be explained by the monomer concentration being below its solubility, so no monomers enter the fibrillar phase. This is called the stable range. The plateau seen to the very right is when the monomer concentration has reached its solubility, meaning that an increase in total Aβ concentration does not lead to an increase in monomer concentration. Instead, the increase is means an increase in fibril concentration. The region in between, seen as a peak between the linear/stable range and the solubility, is the metastable range. Here, the concentration is above the solubility but there has not yet been time for the excess monomer to go into the fibrillar phase. This is the lag phase seen in **Figure 1.3**. The longer the Aβ is allowed to aggregate, the smaller the metastable range is. The different ranges are shown schematically in **Figure 1.5**.

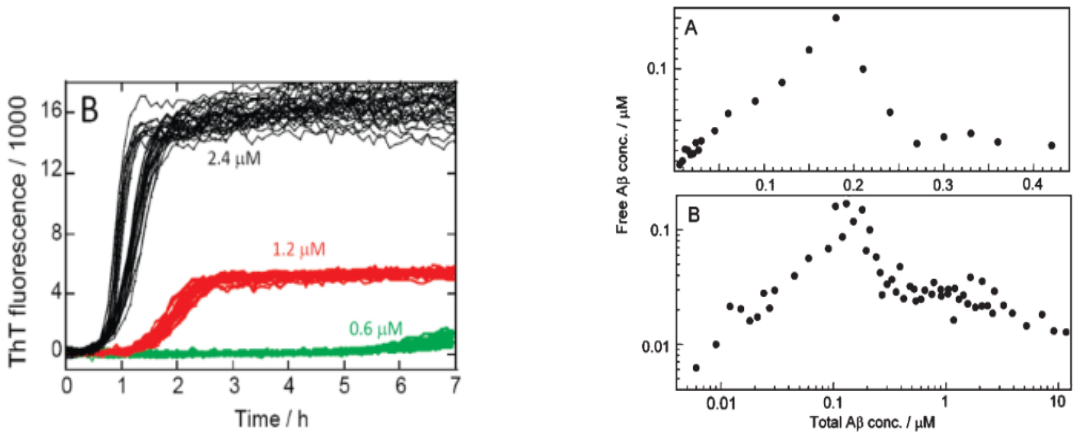

(a) (b)

Figure 1.4: **a)** Aggregation kinetic traces of three different Aβ concentrations, taken from Hellstrand et al. (2009) [8]. **b)** Plot showing total Aβ/free Aβ concentration. From Hellstrand et al. (2009) [8]

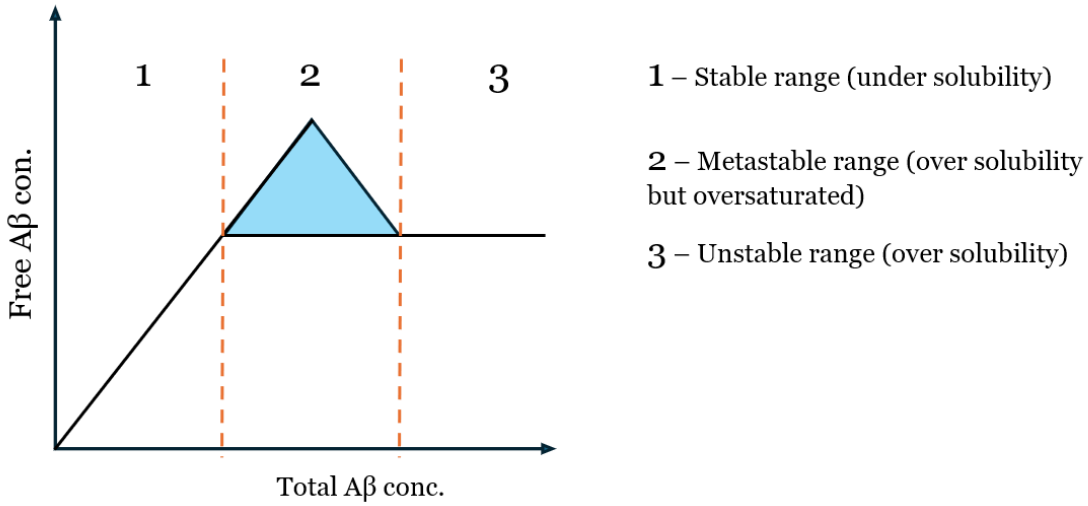

Figure 1.5: Schematic showing the stable, metastable, and unstable ranges of Aβ aggregation.

1.3 ELISA

ELISA stands for enzyme-linked immunosorbent assay, and is a widely used qualitative and/or quantitative detection method that is employed in various fields and research areas. In the context of AD research and diagnostics, ELISA has been a key methodology for the detection of different biomarkers, such as Aβ [13]. There are several subtypes of ELISA. One such subtype is the sandwich ELISA, which is considered the most sensitive [3]. In this subtype, the wells of the ELISA plate first get coated with a capture antibody that binds the antigen of interest. Then, another "layer" of antibody is added, that also binds to the antigen. This is the detection antibody. A way to describe it is that the antigen gets sandwiched between capture and detection antibody. There are several ways that the detection antibody can generate a signal. A common way is to conjugate the detection antibody with horseradish peroxidase

(HRP). Then, after the conjugated detection antibody has bound to the antigen, a chromogenic substrate is added. This substrate, often 3,3',5,5'-Tetramethylbenzidine (TMB), gets oxidised by the HRP and turns the reaction mixture blue [6]. A moment after, a stop solution is added which turns the reaction mixture yellow, which has a maximum absorbance peak at 450 nm [6]. The measured absorbance will be proportional to the amount of antigen. A schematic illustrating the principal behind a sandwich ELISA using a HRP-conjugated detection antibody and TMB can be seen in **Figure 1.6**.

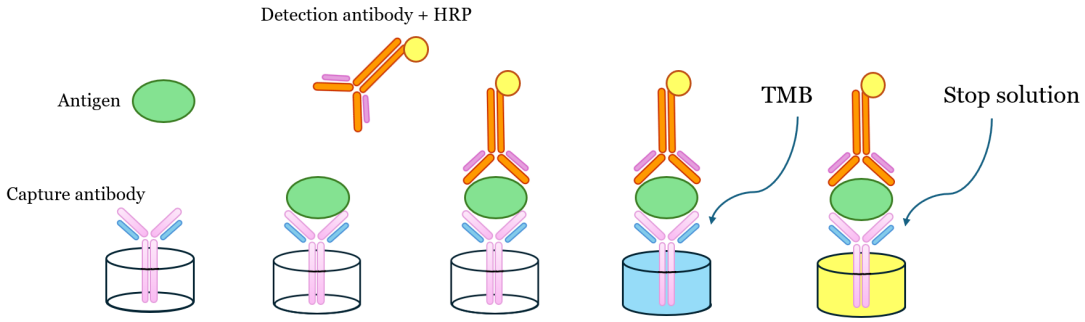

Figure 1.6: Schematic showing the principle behind a sandwich ELISA using a HRP-conjugated detection antibody with TMB as substrate.

The suitability of the ELISA for its intended use is tried with method validation. In ELISA validation, there are a few parameters that are often tried. Three such parameters are sensitivity, specificity, and linearity [12]. Sensitivity can be measured in terms of the limit of detection (LOD) and lower limit of quantification (LLOQ) [12]. LOD is lowest concentration of analyte that can be reliably detected with the ELISA. LLOQ is lowest concentration of analyte that in addition to being able to be detected, can be reliably quantified. There are several ways to calculate these values. Specificity is the assays ability to differentiate between the analyte of interest and all matrix molecules, as well as any related compounds [12]. In the case of an ELISA specific for a type of Aβ, a related compound could be a different type of Aβ. Linearity is when the signal given by a sample is directly proportional to the amount of antigen in the sample [12]. This relation can be described by the equation for a straight line. Linearity is dependent on analyte concentration, and there is a lower and upper concentration value where the relationship is no longer linear. When doing an ELISA, a standard curve is typically made with standards containing known amounts of the analyte of interest. As the aim of this project is to develop an ELISA for monomeric Aβ42, a standard curve will be made with monomeric Aβ42.

1.4 SEC

To obtain monomeric Aβ42, it must be separated from other species such as oligomers and fibrils. One method of doing so is to put purified Aβ42 through size exclusion chromatography (SEC). SEC is a method which separates biomolecules based on molecular size differences [7]. The separation can be monitored with a chromatogram, where different peaks represent the elution of species with different molecular weight. Knowing which peak represents the monomer fraction, it is possible to collect the monomers

once the peak is seen on the chromatogram. **Figure 1.7** shows two examples of such chromatograms, published by Linse (2020) [9].

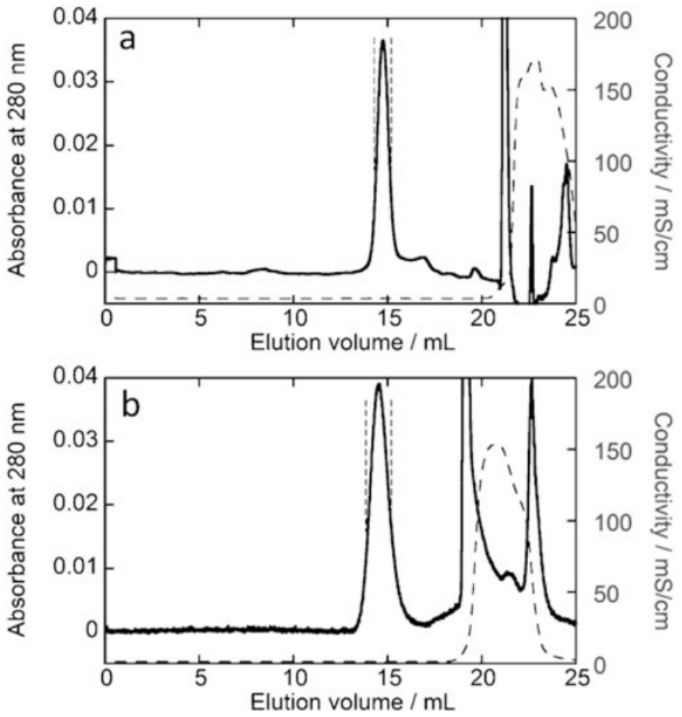

Figure 1.7: Typical chromatograms for SEC purification of Aβ. **a)** shows the chromatogram from a column with increased performance compared to **b)**. The vertical dashed lines indicate the monomer peak. [9]

1.5 Project goals and research questions

As stated in the beginning of the introduction, this project aims to develop an ELISA for monomeric Aβ42 that can be used in experiments investigating the solubility of Aβ42, and how the solubility is affected by different conditions and environments. The ELISA will be based on a sandwich ELISA method described in Hellstrand et al. (2009). The protocol will be followed and the same buffers and solutions will be used to the extent that it is possible. However, the capture and detection antibody will not be the ones used in Hellstrand et al. (2009). Instead, appropriate candidates will be ordered and their suitability tested. The ELISA should be satisfactory in terms of sensitivity and specificity. During the planning phase of the project, it was decided that a linear range of down to 10 nM (or lower) would be desirable. The assay will be tried with monomeric Aβ40 and Aβ42 fibrils to test the specificity. Ideally, there should be no cross-reaction with monomeric Aβ40 or Aβ42 fibrils. The aggregation experiments described in Hellstrand et al. (2009) should be repeated to see if the same results are achieved. Finally, the assay should be tested with a CSF-environment instead of buffer, to see if it has an effect on the measurement.

2 Methods

2.1 Method overview

To achieve the project goal and answer the research questions, a number of ELISAs were done. The protocol was based on a method previously described in Hellstrand et al. (2009). Firstly, assays were done to determine the suitability of the antibody candidates, solutions, buffers and other materials. The method was also validated by testing the sensitivity, specificity and other method validation characteristics. Once the method was validated, the assay was used for different applications. This included measuring Aβ42 concentration in CSF, and an attempt to recreate the the results obtained in the Hellstrand paper. All experiments followed the same general protocol, which is described in section 2.2. Information about how the specific experiments were done that is not found in the general protocol, can be found under their specific sections. If there are any deviations from the general protocol it will also be described under the sections for the specific experiments.

2.2 General Protocol

2.2.1 Protein Processing and Protein Standards

For every ELISA, a series of protein standards with known Aβ42 concentrations were made to create a standard curve. The protein standards were created from purified Aβ42 protein, produced as previously described [9]. Firstly, the protein was allowed to dissolve in Gu6 (*Gu6: 6 M guanidinium hydrochloride (GuHCl), 20 mM sodium phosphate, pH 8.5)* for 15-30 min. The protein was then put through SEC on an (*Superdex 75 Increase column, 20mM sodium phosphate buffer (pH 8.5), 200uM EDTA, 0.02% NaN_3*). The monomer fraction was collected from the center of the monomer peak and put on ice. The collected protein was aliquoted into appropriate amounts and frozen at -80°C. The concentration of the protein was calculated by taking the average absorbance of the peak and using Beer Lambert's law; **Equation 2.1**. The molar absorption coefficient of Aβ is $1440 M^{-1} cm^{-1}$, and l is the path length specific to the instrument used.

$$A = \epsilon \cdot c \cdot l \tag{2.1}$$

Having calculated the protein concentration, a series of protein standards were made by diluting the aliquotes of the purified protein in sodium phosphate buffer with 0.2% BSA. BSA is a blocking agent that prevents non-specific binding.

2.2.2 ELISA Protocol

Firstly, 100 μL of capture antibody(*BioLegend® Purified anti-β-Amyloid 1-42 Antibody, clone 12F4, 2.5μg/ml in 30 mM $NaHCO_3$, pH 9.6, 0.05% NaN_3 bicarbonate buffer*) was added to the wells of a 96-well plate (*invitrogen, Nunc MaxiSorp™ Flat-Bottom Plate*). The plate was covered and allowed to incubate overnight at 4°C with rocking. Then, the plate was washed twice with PBS*(*6 mM sodium phosphate, 137 mM NaCl, 3 mM KCl, pH 7.4*), before adding 200 μL of gelatin blocking buffer(*SIGMA® Gelatin blocking buffer*) to each well. The plate was then allowed to incubate for 4-7** hours at room temperature and with rocking. Following the incubation, the blocking solution was dumped and 50 μL of sodium phosphate buffer immediately added, to prevent the wells from drying out. 100 μL of blank(sodium phosphate buffer), standard or sample was added to each well. Each standard/sample/blank was added in triplicates. Then, the plate was incubated overnight at 4°C with rocking. After, the plate was washed twice with PBST(*PBS with 0.05% Tween 20*) and once with PBS. 100 μL of detection antibody(*BioLegend® HRP anti-β-Amyloid 1-16 Antibody, clone 6E10, 1:4000 dilution in 5% BSA sodium phosphate buffer*)*** was added and allowed to incubate for four hours at room temperature and rocking. The plate was then washed again twice with PBST and once with PBS. After that, 100 μL substrate(*Thermo Scientific™, 1-Step™ TMB ELISA Substrate Solutions*) was added to each well and allowed to react for two minutes. The reaction was then stopped with 100 μL of stop solution(*5.8% o-phosphoric acid*) in each well. The absorbance was read at 450 nm. A schematic describing the workflow is presented in **Figure 2.1**.

**Note about PBS: Different brands of PBS tablets were used to make PBS. This means that there might be slight differences in the concentrations of the components of the PBS*

***Note about blocking incubation time: The aim was to have a incubation time of 4 hours, but that was sometimes exceeded. The longest was around 7 hours.*

****Note about detection antibody: The aim was to add 5% BSA to the detection antibody. However, for some experiments the concentration was 0.2% and for some there was no BSA.*

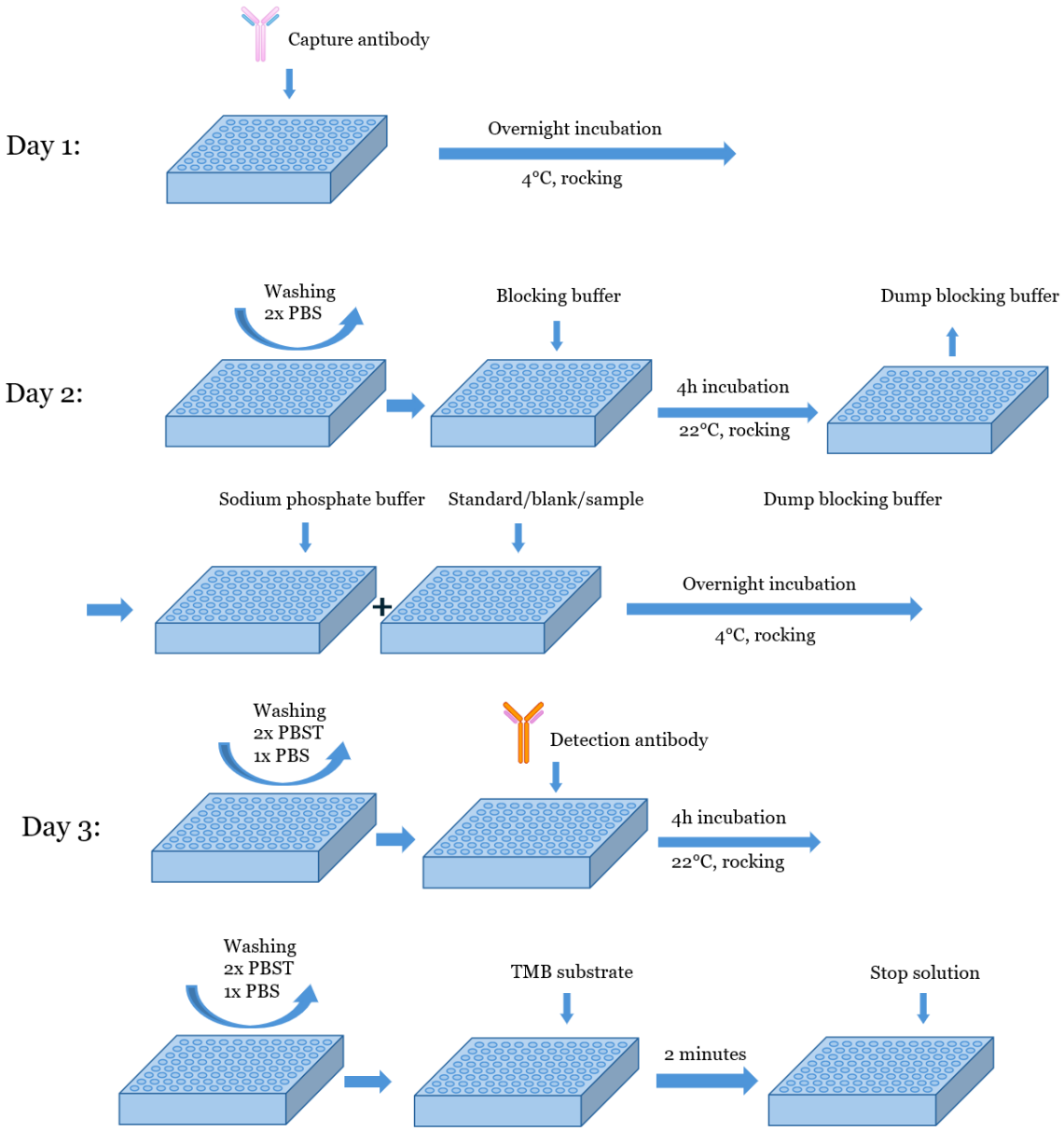

Figure 2.1: A schematic of the ELISA workflow. The tasks are divided by which day they are performed.

2.2.3 Data Analysis

The absorbance data was imported into MATLAB. There, the mean of all triplicates were averaged and error was calculated using the standard deviations. The mean value of the blanks was subtracted from the mean of the standards/samples. Then, the blank corrected mean absorbance values of the protein standards were plotted against their known concentration to create a standard curve. It was found that taking the natural logarithm of the concentration and plotting that against the absorbance values produced the best curves. A linear regression was made of the linear part of the standard curve. The resulting linear equation could be used to calculate the concentration of samples with unknown amounts of Aβ42.

2.3 Method Validation Experiments

For the method validation experiments, there were no samples tested with the ELISA, only protein standards to create standard curves. The protein standards were prepared as described in section 2.2.1. With the data from the standard curves, the sensitivity and linearity of the method could be determined. LOD and LLOQ were calculated according to **Equation 2.2** and **Equation 2.3**. $c_{blank\ signal}$ denotes the concentration at which the signal is equal to the mean signal of the blank. σ_{blank} is the standard deviation of the blank.

$$LOD = c_{blank\ signal} + 3\sigma_{blank} \tag{2.2}$$

$$LLOQ = c_{blank\ signal} + 10\sigma_{blank} \tag{2.3}$$

The Aβ-42 specificity of the capture antibody was tested by doing two protein standard curves, one with Aβ42 and one with Aβ40. The Aβ40 was purified and the monomer isolated as previously described [9]. For comparison, the same concentrations of protein standards were used.

Additionally, the specificity for Aβ42 monomer versus Aβ42 fibrils was also investigated. The fibrils were made at 37°C in *20 mM NaP, pH 8.0, 0.2 mM EDTA, 0.02% NaN_3 and in Maxymum recovery tubes (Axygen, ref. MCT-150-L-C)* . Before adding them to the plate, they were first centrifuged twice; for 20 minutes, at 18000g and 37°C. The supernatant was discarded after each centrifugation. After that, they were sonicated for 2 minutes. The fibrils were then diluted with sodium phosphate buffer with 0.2% BSA to desired concentrations. To test if there were any clumps of fibrils, the ThT-fluorescence was measured for a few concentrations. If there was a linear relationship between fibril concentration and ThT-fluorescence, it meant that the sonication had removed any potential clumps. The ThT-fluorescence was measured by adding the chosen fibril concentrations to a clear bottom plate (*CORNING Costar®Assay Plate, 96 Well, 3631*) along with a few μL of ThT. The fluorescence was read at 280 nm.

A comparison was made between the capture antibody mentioned in the protocol (*BioLegend®Purified anti-β-Amyloid 1-42 Antibody, clone 12F4, 2.5mg/ml in bicarbonate buffer*) and a second antibody (*Sigma-Aldrich®Anti-Amyloid β42 Antibody, clone G2-11, 2.5mg/ml in bicarbonate buffer*). To compare the two, two standard curves were made using the respective capture antibody.

2.4 CSF experiments

Two spike-experiments with CSF were done. They consisted of taking CSF and adding a known amount of Aβ42. The resulting absorbance value could then be compared to that of a protein standard with the same concentration. The two experiments were done the same way, except that the first experiment had three spiked CSF concentrations, and the other only had one. The CSF was provided as part of an ethically

approved study, see the ethical statement in section 5. The CSF was pooled from patients with excessive volumes of CSF, and their status in regards to neurodegenerative diseases is unknown. The CSF was used unprocessed for the two spike-experiments, save for a 30 second vortex for the first experiment. In the second experiment, this step was forgotten.

2.5 Kinetic experiment

To attempt to recreate the results in the Hellstrand paper, which the method was based on, an aggregation kinetics experiment was set up. For this experiment, a new batch of Aβ42 was purified using SEC. The Aβ42 was diluted to 11 concentrations of monomer between 5 and 0.005 μM, with a dilution factor of 2. The 11 protein solutions were added to a clear bottom plate, in triplicates. For the three highest concentrations (5, 2.5 and 1.25 μM), two sets of triplicates were made. There were also two sets of blank-triplicates. For each of the three concentrations, and blank, ThT was added to one set of triplicates. The plate was placed in a plate reader and the protein was allowed to aggregate for roughly 21 hours. This is different to the Hellstrand method, were the aggregation was allowed to proceed for 84 - 96 hours. The concentrations with added ThT were used to track the aggregation, meaning that the ThT-fluorescence was measured during the aggregation. After 21 hours, the protein solutions were collected from the wells and centrifuged for for 20 minutes, at 18000g and 37°C. The supernatants were collected and added to an ELISA as samples. The ELISA was done as described in the ELISA protocol. A standard curve was made. Using the standard curve, the concentration of monomer that was left in the supernatant after aggregation could be calculated. This concentration was then compared to the total Aβ42 concentration, meaning the concentration of the protein solution before aggregation. The fluorescence values generated by the ThT where imported into MATLAB, so that a kinetic trace graph could be done.

3 Results

3.1 Method Development and Validation

3.1.1 Linearity and Sensitivity

Firstly, an assay testing the chosen components of the ELISA was done to see if they would give a satisfactory standard curve. As can be seen in **Figure 3.1 a)**, the protein standards, ranging from 0.24 to 1000 nM Aβ42, gave rise to a negative exponential curve after absorbance was measured. To more easily see a potential linear range, the natural logarithm of the concentration was plotted instead of the real concentration. This is shown in **Figure 3.1 b)**. The fourth lowest concentration, 15.6 nM, appears to be an outlier since it does not fit in with the general trend created by the other concentrations. This made it so a linear range could not be easily determined.

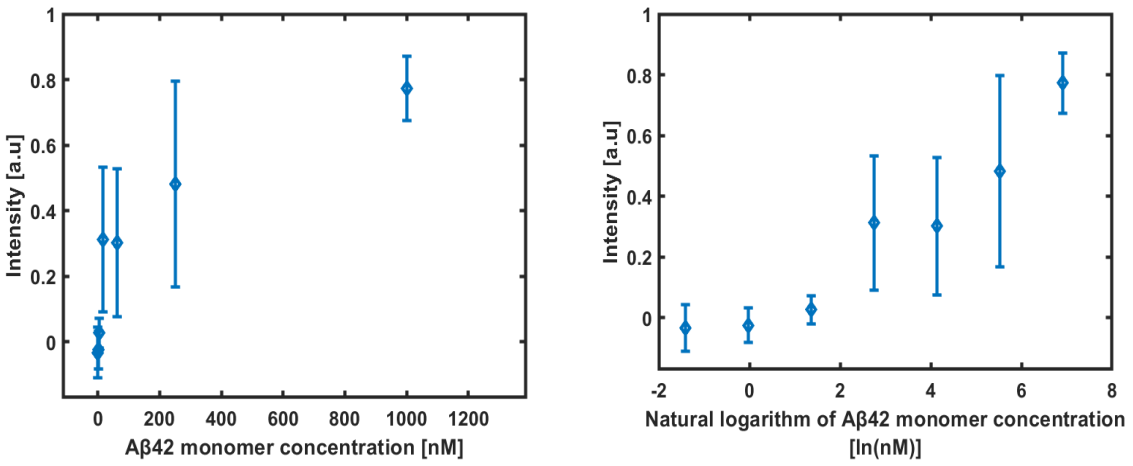

(a) **(b)**

Figure 3.1: The measured absorbance intensity [a.u] of six Aβ42 protein standards.The Aβ42 concentrations are as follows: 1000, 250, 62.5, 15.6, 3.9, 0.98, 0.24 nM. **a)** Concentration plotted as real concentration. **b)** Concentration plotted at natural logarithm of real concentration

The results from the initial test showed that an extended concentration range would be necessary to accurately determine the linear range. It was found that a concentration range between 0.01 to 100 nM Aβ42 produced satisfactory curves; the linear range was seen, and had "tails", meaning the curve was flattened before and after the linear range. The first experiment to yield such a curve is presented in **Figure 3.2 a)**. However, as time went on and more experiments were made, the overall intensity of the assay decreased and the shape of the standard curve changed. The graphs in **Figure 3.2 a)**, **b)**, and **c)** show this decline. Note that in **a)** and **c)** the full range of 0.01 to 100 nM concentration range was used, while in **b)** the range was 0.3 to 31.6 nM. From **a)** to **c)** the highest intensity measured goes from 0.35 to under 0.06, and the standard curve has lost its shape with the linear region and tails, between **a)** and **c)**. These graphs are the results of equivalent experiments and were done approximately 2

weeks apart from each other. After some experimenting, the graph in **d)** was obtained by making all fresh new buffers and solutions. Previously, the same sodium phosphate buffer had been used every week. After making fresh buffers, the appearance of the standard curve was back to what was observed in **a)**.

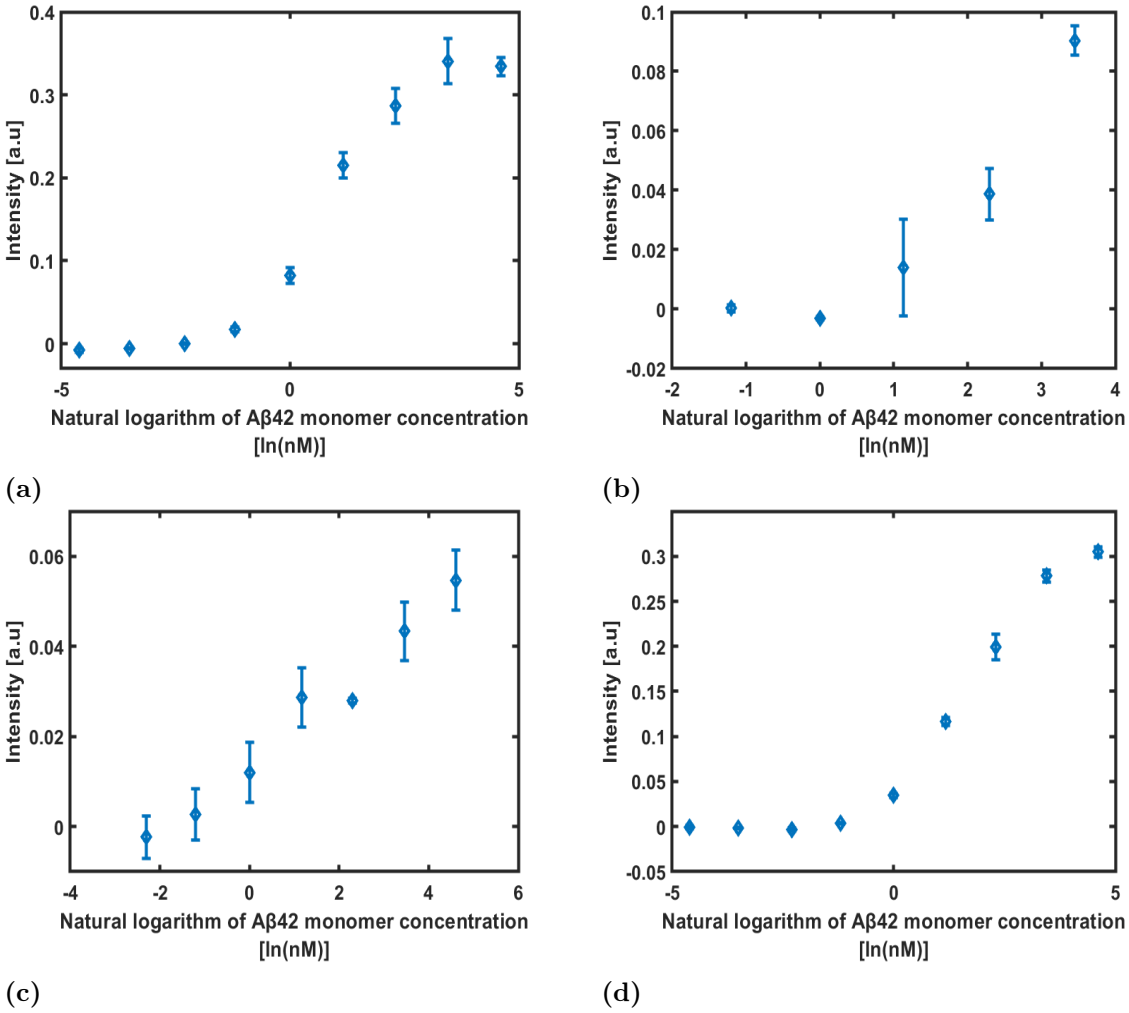

Figure 3.2: Standard curves for four different experiments. From **a)** to **b)** a decline in standard curve quality can be seen, due to the buffers used getting old. **d)** shows a standard curve made with fresh buffer.

Now with two satisfactory standard curves, the linearity, range and limits of quantification were determined. Looking at the curves, the linear range appeared to be between 1 and 31.6 nM. In **Figure 3.3 a)** and **c)** the two standard curves are shown again with these concentrations marked in red. To the right of the standard curves, in **Figure 3.3 b)** and **d)**, are linear regressions made of the visually estimated linear ranges. Both regressions show good linearity, in particular the one in **d)** has a R^2 value of very close to 1.

From these two experiments the LOD and LLOQ were determined. They are presented in **Table 3.1**. The values differ slightly, but it can be seen that both the LOD and LLOQ fall somewhere in the low single digit nM range.

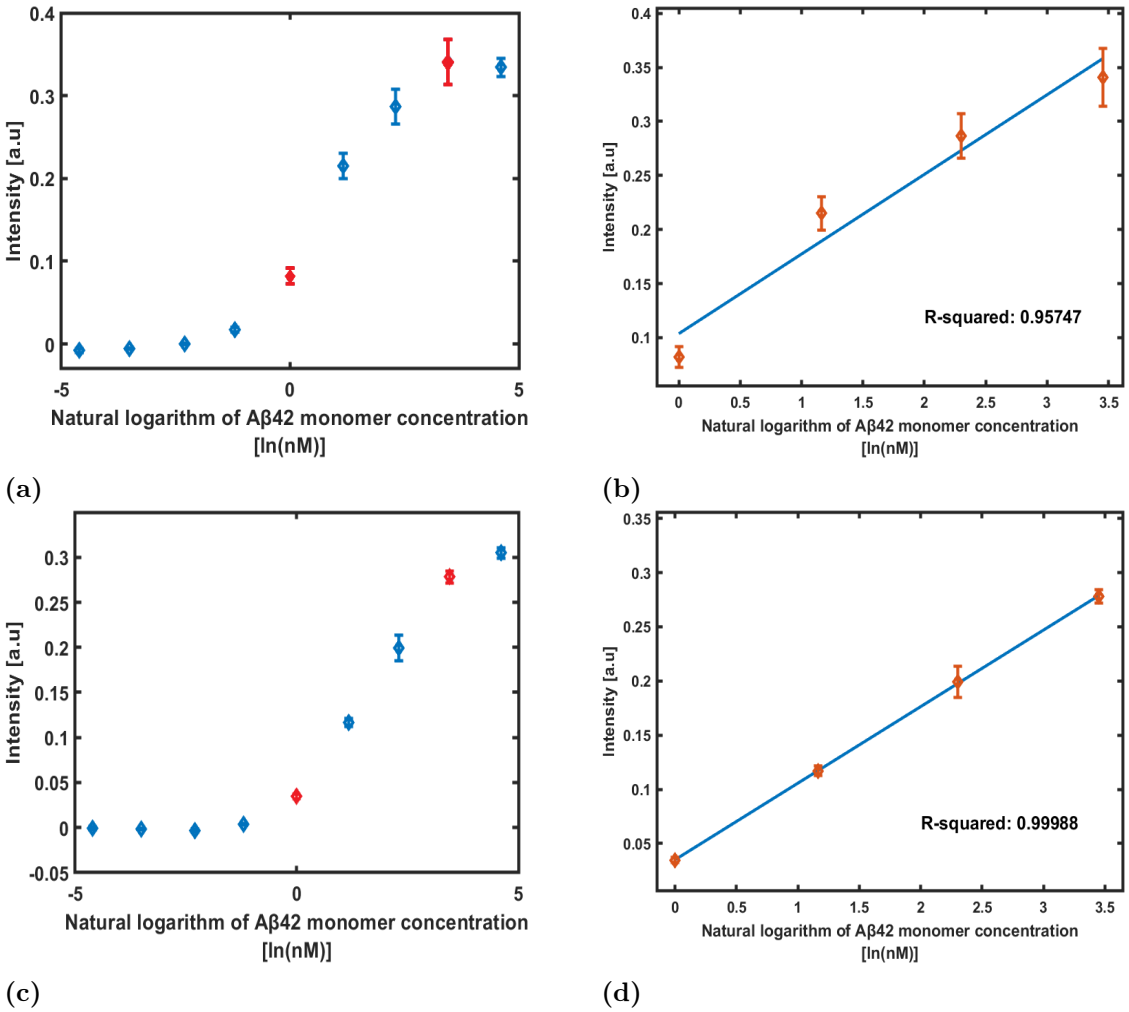

Figure 3.3: **a)** Standard curve obtained with the following concentrations: 100 nM, 31.6 nM, 10 nM, 3.2 nM, 1 nM, 0.3 nM, 0.1 nM, 0.03 nM, 0.01 nM. Points marked in red indicate the start and end of the linear region. **b)** A linear regression made from the range of concentrations indicated in a); 31.6 nM, 10 nM, 3.2 nM, 1 nM. **c)** Another standard curve obtained with the same concentrations presented in a). The red points indicate the linear range. **d)** A linear regression made from the linear range in c). The goodness-of-fit, R^2, of the linear regressions are presented in b) and d).

Table 3.1: The linear range and the calculated LOD and LLOQ for the standard curves shown in Figure 3.2 a) and d), here called experiment A and B respectively.

Experiment	Linear range	LOD	LLOQ
A	1 - 31.6 nM	1.4 nM	3.9 nM
B	1 - 31.6 nM	3.0 nM	5.5 nM

3.1.2 Specificity

The specificity of the capture antibody between Aβ42 and Aβ40 as well as the specificity between Aβ42 monomer and Aβ42 fibril was investigated. Comparing the Aβ42 and Aβ40 standard curves in **Figure 3.4**, it can be seen that all concentrations of Aβ40 resulted in an absorbance intensity very close to zero, indicating that the capture antibody does not cross-react with Aβ40.

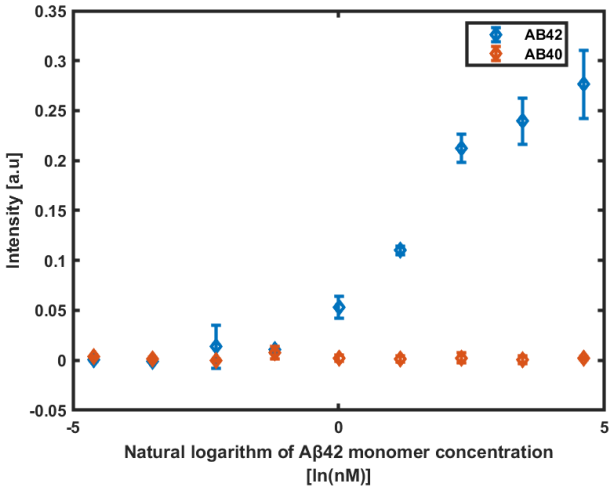

Figure 3.4: Comparison between a standard curve made with Aβ42 (blue), and a standard curve made with Aβ40 (orange). Both standard curves have the same concentrations; 100, 31.6, 10, 3.2, 1, 0.3, 0.1, 0.03, and 0.01 nM.

The results from the experiments comparing monomer and fibril are a bit more unclear. In **Figure 3.5** two such experiments are shown. In **Figure 3.5 a)** an experiment with the standard curve with 100, 31.6, 10, 3.2, 1, 0.3, 0.1, 0.03, and 0.01 nM protein standards is shown with three different fibril concentrations; 1000, 600, 200 nM. It can be seen that the fibrils did give signal, however their signal is a bit lower than what would be expected of monomer of the same concentration. In **Figure 3.5 b)** another experiment is shown with the standard curve with 31.6, 9.9, 3.1, 1, and 0.3 nM. The three fibril concentrations are 150, 75, and 37.5 nM. In this experiment, the fibril also gave signal, but in this case the difference in signal between the fibrils and signal for equivalent monomer concentration is bigger. Note that these experiments were done before the issue with the freshness of buffers was discovered, which is why the shapes of the standard curves, especially the one in **b)**, look different to the ones previously shown.

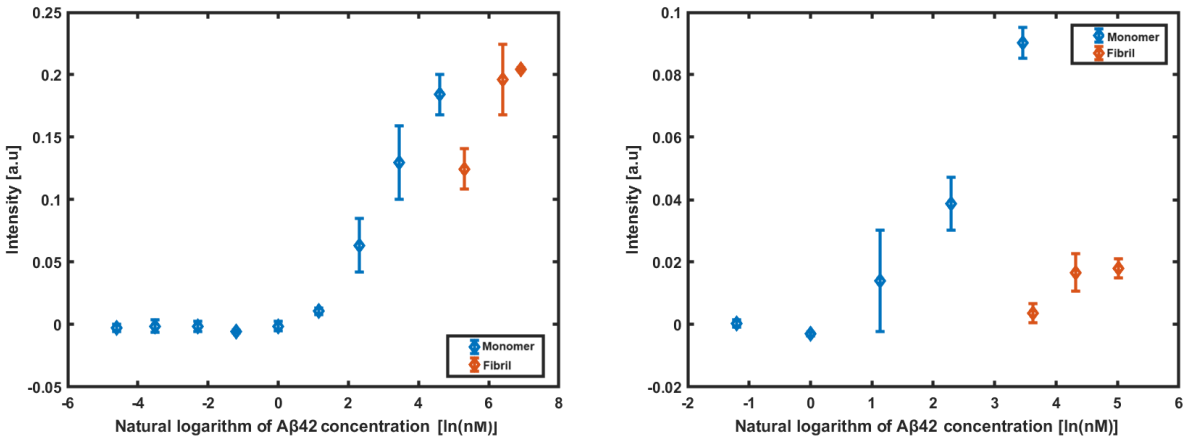

(a) **(b)**

Figure 3.5: Experiments testing the cross-reactivity of the capture antibody with Aβ42 fibrils. In **a)**, the standard curve (shown in blue) is made up of protein standards with the following concentrations: 100, 31.6, 10, 3.2, 1, 0.3, 0.1, 0.03, and 0.01 nM. The three fibril concentrations used (in orange) were 1000, 600, 200 nM. In **b)**, the standard curve included 31.6, 9.9, 3.1, 1, and 0.3 nM and the fibril concentrations 150, 75, and 37.5 nM.

3.1.3 Choice of capture antibody

As mentioned in the method section, two different capture antibodies were tested; (*BioLegend® Purified anti-β-Amyloid 1-42 Antibody, clone 12F4*) and (*Sigma-Aldrich® Anti-Amyloid β42 Antibody, clone G2-11*). The standard curve made with each antibody is shown in **Figure 3.6**. The G2-11 clone did not produce significant signal for any concentration in the standard curve. The G2-11 clone was not used in any other experiments.

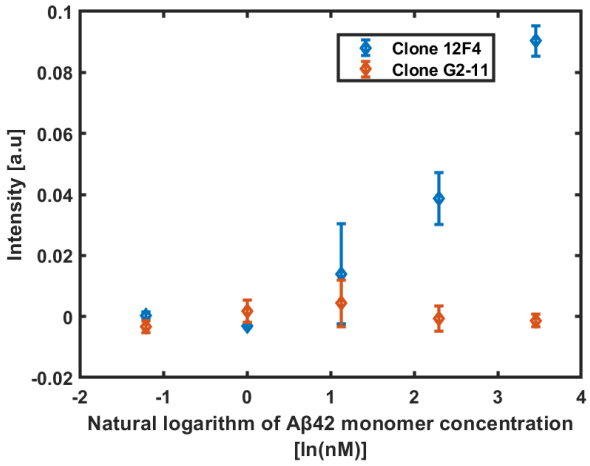

Figure 3.6: ELISA standard curves done with two different clones of capture antibody; Clone 12F4 (blue) and clone G2-11 (orange). Both standard curves include the standard concentrations 31.6, 9.9, 3.1, 1, and 0.3 nM.

3.2 CSF experiments

There were two CSF experiments done. In the first one, CSF was spiked with Aβ42 into three different concentrations; 100, 17.9, and 3.2 nM. The result from this experiment is shown in **Figure 3.7 a)**. It can be seen that the spiked CSF gave a lower signal as compared with equivalent concentrations of Aβ42 in the standard curve. In **Figure 3.7 b)** the result of the second experiment which included one concentration, 10 nM, of spiked CSF is shown. The same concentration of protein standard, which is represented by the blue point above the orange point for CSF, gives a higher signal. Both experiments thus showed a lower signal of Aβ42 in CSF as compared to the same concentration in sodium phosphate buffer.

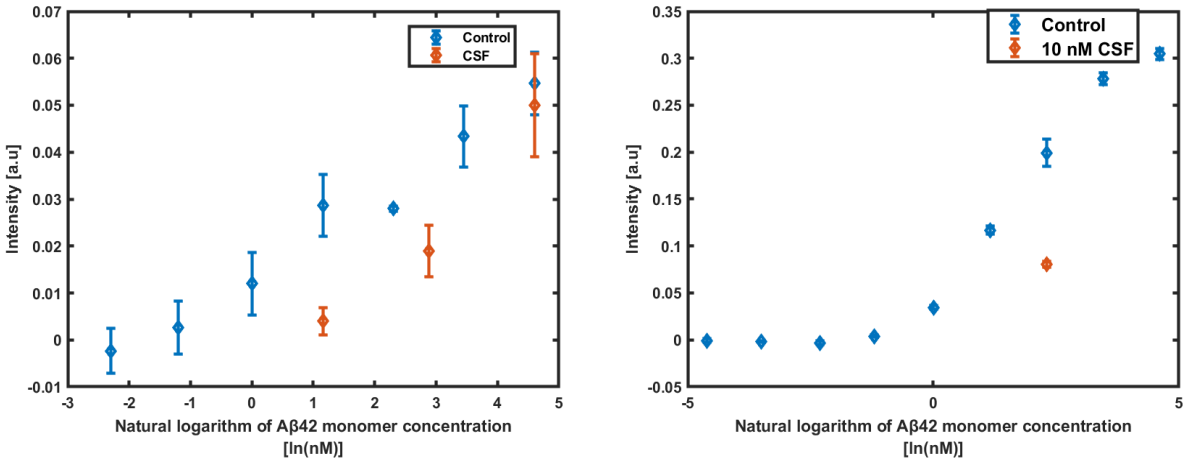

(a) **(b)**

Figure 3.7: Results from two experiments comparing standard curves of Aβ42 in buffer with Aβ42 in CSF. The standard curves are shown in blue while the spiked CSF is shown in orange. **a)** Concentrations in standard curve: 100, 31.6, 10, 3.2, 1, 0.3, 0.1 nM. CSF with spiked concentrations: 100, 17.9, and 3.2 nM Aβ42. **b)** Concentrations in standard curve: 100, 31.6, 10, 3.2, 1, 0.3, 0.1, 0.03, and 0.01 nM. The spiked CSF concentration is 10 nM.

3.3 Kinetic Experiment

The results from the kinetic experiment include the kinetic traces produced by the ThT fluorescence during the aggregation, and ELISA measurements of monomer concentration after aggregation. The kinetic traces produced are shown in **Figure 3.8**. The Aβ42 was allowed to aggregate for roughly 21 hours, however at around 10 hours there was an issue with the instrument tracking the ThT fluorescence. For some unknown reason an error was produced that stopped the instrument from tracking the fluorescence between hour 10 until it was manually started again at hour 17. This is seen as the gap in **Figure 3.8 b)**. **Figure 3.8 a)** shows the experiment cut out at 10 hours. It can be seen that the 5μM aggregation reached the plateau at around 3 hours, while the 2.5μM reached the plateau at around 6 hours. The 1.25μM concentration seems to have entered the exponential phase somewhere between 15 and 20 hours, seen be the slight upwards curve in **Figure 3.8 b)**.

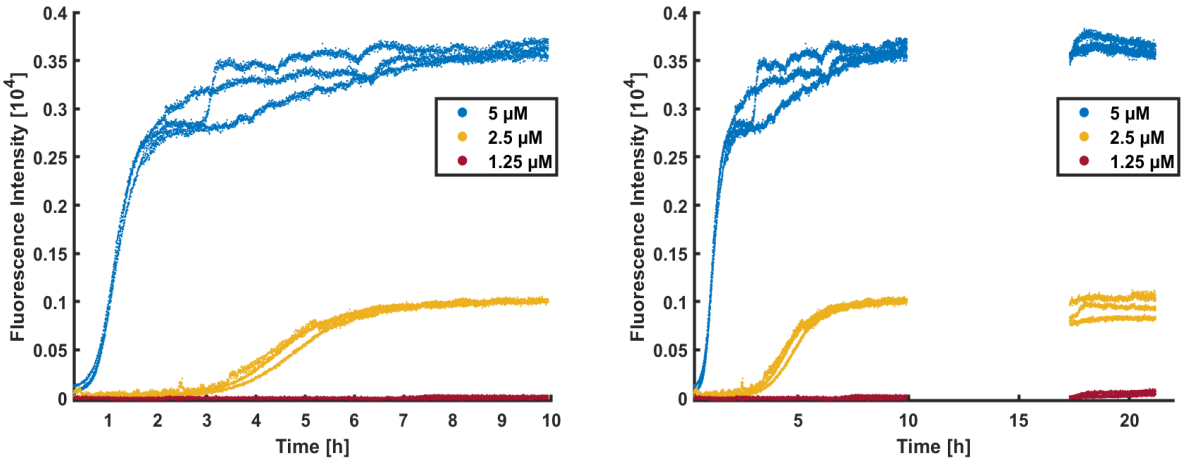

Figure 3.8: Kinetic traces for aggregation of 5μM, 2.5μM, and 1.25μM Aβ42, during **a)**, the first 10 hours and, **b)**, the whole roughly 21 hours of the experiment.

For the monomer collected after aggregation, an ELISA was made. The standard curve of this ELISA is seen in **Figure 3.9**. The standard concentration of 0.4 nM seems to not fit in with the rest of the points. This makes it difficult to do a linear regression, which is needed to be able to calculate the concentration of the collected monomer. The previous ELISAs done had shown high similarity in how the standard curves looked, therefore it seemed reasonable to treat the 0.4 nM concentration as an outlier and remove it, in order to get the familiar shape of the standard curve. The standard curved with the 0.4 nM concentration removed is shown in **Figure 3.9 b)**. Then, the concentrations of monomer (free Aβ) could be calculated. These concentrations are plotted against total Aβ and presented in **Figure 3.10**. **Figure 3.10 a)** shows the un-averaged result from the triplicates while **Figure 3.10 b)** shows the average of the triplicates. **Figure 3.11** shows the averaged results overlaid with data points from the same experiment conducted by Hellstrand et al. (2009), which was presented in the introduction. It can be seen that they have similar linear/stable ranges, however it seems that the slope of the linear range from this experiment is a little less than 1. The metastable region seen in the Hellstrand et al. (2009) experiment is not seen in this experiment. The solubility, meaning the plateau seen to the right, is found to be at a higher monomer concentration compared to Hellstrand et al. (2009).

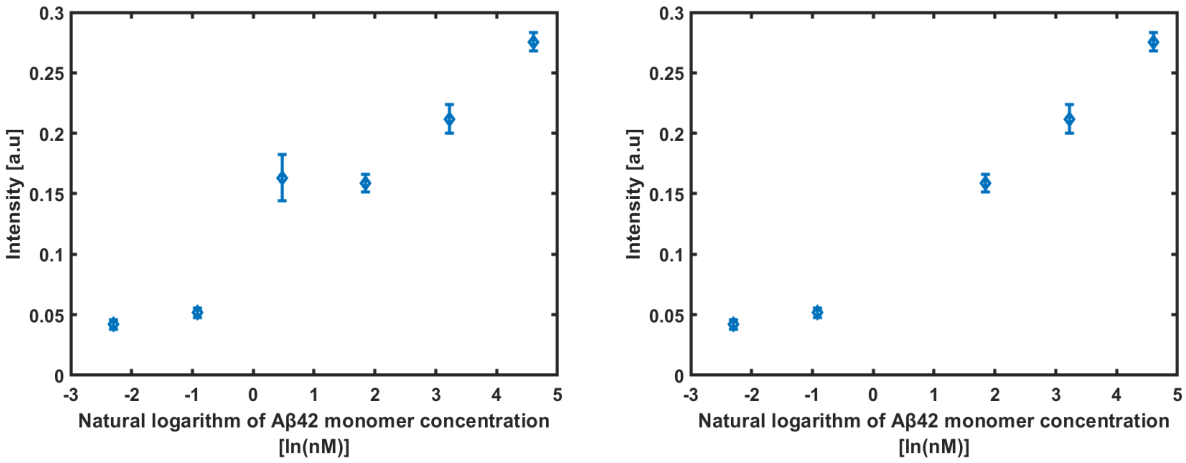

(a) (b)

Figure 3.9: The standard curve created for monomer in the kinetic experiment. **a)** shows the curve with all concentrations present; 100, 25.1, 6.3, 1.6, 0.4, and 0.1 nM. **b)** shows the standard curve with the 0.4 nM concentration removed.

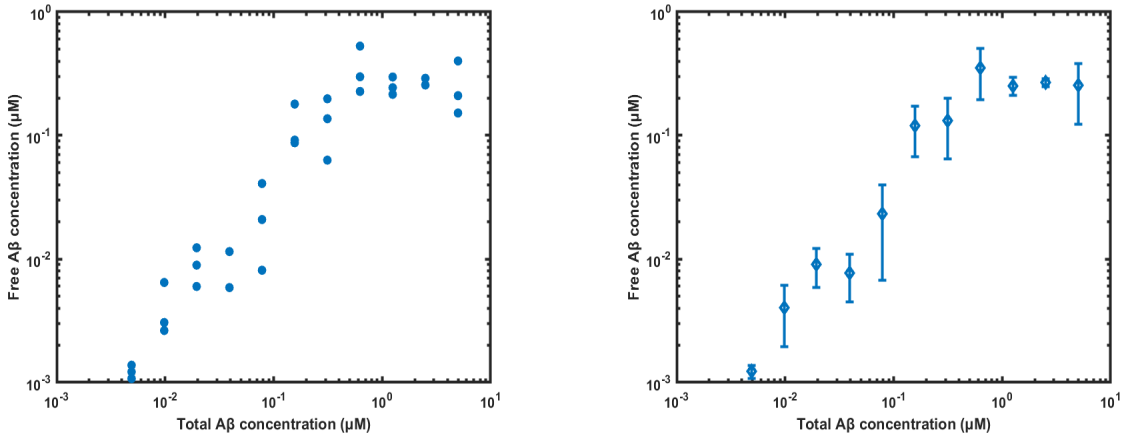

(a) (b)

Figure 3.10: Total vs free Aβ42 plots produced from the aggregation kinetics experiment. **a)** shows the result from all triplicates while **b)** shows the averaged result.

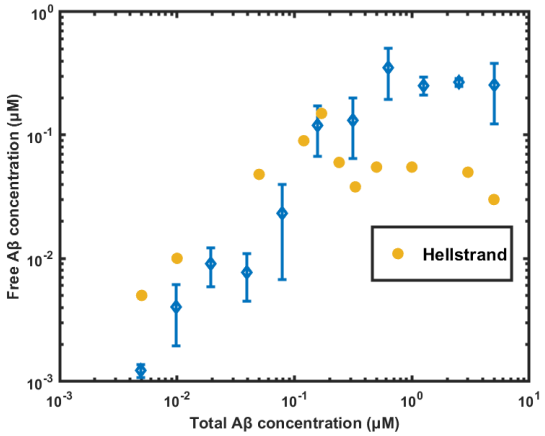

Figure 3.11: Total Aβ42/free Aβ42 plot, overlaid with data points from the same plot in the Hellstrand et al. paper (2009) [8].

4 Discussion

4.1 Development of Method

The goals of the method development was to develop an ELISA method based on a previous method described in Hellstrand et al. (2009), that a linearity of the standard curve down to at least 10 nM should be achieved, and that the method should be specific for Aβ42 monomer.

The goal of the linearity was achieved since the linearity was shown to go down to single digit nM. Of course, the linear range differs slightly between each experiment, since the standard curve is sensitive to things such as buffer freshness. Nonetheless, achieving linear ranges below 10 nM using this method was shown to be possible. For quantification, the LLOQ landed somewhere around 5 nM, which is a satisfactory limit. The upper limit of detection, linearity, or quantification is not as important since samples can always be diluted to a lower concentration.

The specificity for Aβ42 over Aβ40 was good. That makes this a good method for determining the Aβ42 concentration in samples where both Aβ42 and Aβ40 could be present, for example in some biological samples. The method showed some cross-reactivity with Aβ42 fibrils, which was not desirable. However, there was still a preference for the monomer species, and it seems like the preference is stronger when the fibril concentration is low. Additionally, for many experiments there is a sample preparation step where the fibrils and monomers are separated, which makes the cross-reactivity less of an issue. It should be noted that there is some uncertainty with the results from the fibril experiments. As there is an overnight incubation at 4°C, there is a possibility that some fibrills have reversed into the monomer phase, meaning that what appeared to be fibrils being detected, was in actuality monomers.

In the methods section, there were some notes about inconsistencies in PBS composition, blocking incubation time, and the BSA concentration mixed with the detection antibody. The PBS composition should not have a significant effect on the experiments, since it is only used for washing and the compositions were very similar. The blocking incubation time might have an effect on the sensitivity of the ELISA, since blocking prevents non-specific binding, but it is unclear if a few extra hours of blocking time has any effect. The different BSA concentrations with the detection antibody, 5% or 0.2%, have a potential effect on the sensitivity, since BSA is an blocking agent, but to what degree is not clear. Experiments using both concentrations had satisfactory sensitivity, but 5% is probably the better concentration since it theoretically should give a higher sensitivity. What can be said about the sensitivity for certain, is that it is important to use fresh buffers and solutions, as not doing so was seen to have a clear negative effect on the sensitivity and the linearity of the standard curve.

4.2 CSF environment instead of buffer environment

From the results of the CSF experiments, it seems that the CSF environment is interfering with the ELISAs ability to measure the Aβ42 monomer concentration. It is likely something in the CSF that is interfering with the ability of the capture antibody to bind with Aβ42. It is not something in the CSF that is affecting the absorbance readout since the CSF matrix is washed away before the absorbance is read. Possible future experiments could involve investigating if there is some processing step of the CSF that removes this interfering effect. It could also be interesting to see how diluting the CSF to different dilutions affects the interference.

4.3 Kinetics experiment

The aggregation experiments described in Hellstrand et al. (2009) were repeated in a similar experiment. The kinetic traces showed less aggregation compared to aggregation of similar concentrations in the Hellstrand paper. However, this might be explained by the fact that the aggregation time for this experiment was shorter. The total Aβ42/ free Aβ42 plot looked different compared to the Hellstrand plot. The stable range did not produce a slope that was equal to 1, it was somewhat lower, which indicates that some monomer has been lost in the process. This might because of adsorption of monomer to surfaces, for example. There was no metastable region, and the solubility (the plateau) was reached at a higher monomer concentration compared to Hellstrand. It should be noted that the six highest concentrations, being the concentrations in the plateau, had calculated monomer concentrations that were above the highest concentration of the standard curve. This makes the result uncertain. Since the ELISA is known to become saturated above the linear range (seen by a "tail" nearing a constant absorbance intensity above the linear range), it means that differences in concentration at high concentrations can not be seen. Therefore, the plateau seen might not be because of an equilibrium being reached, but rather that the ELISA is saturated. To avoid this uncertainty, a future repeat of this experiment could be made with more dilutions of the samples, to ensure that the concentrations fall within the linear range.

There is a possibility that the shape of the Aβ42/free Aβ42 plot is not due to the ELISA being saturated. In that case, the absence of metastable range, and higher solubility compared to Hellstrand could be because the formation of fibril reached in this experiment is of a different type, that is easier and faster to reach (no metastable region) with higher solubility.

4.4 Conclusions

It can be concluded that the method development was a success. This is motivated by the method having a satisfactory sensitivity, and specificity, since the cross-reactivity with fibrils can be worked around. An important takeaway from the method development is that it is very important to use fresh buffers. As desired, the aggregation experiments described in the Hellstrand paper were able to be replicated, however with some differing results. The effect of the CSF environment was able to be studied, and it was concluded that CSF probably has some inhibitory effect on the assay.

5 Ethical Statement

The CSF used in this project was received by the department as part of the BioFINDER 2 study (www.biofinder.se). The study was done according to the Helsinki Declaration and all patients gave written consent prior to donating the CSF. The study was approved by the ethics committee at Lund University (Dnr 2016/1053).

Bibliography

[1] M. Ahmed, J. Davis, D. Aucoin, T. Sato, S. Ahuja, S. Aimoto, J. I. Elliott, W. E. Van Nostrand and S. O. Smith, "Structural conversion of neurotoxic amyloid-1–42 oligomers to fibrils", *Nature Structural & Molecular Biology*, vol. 17, no. 5, pp. 561–567, May 2010, ISSN: 1545-9993, 1545-9985. DOI: 10.1038/nsmb.1799. [Online]. Available: https://www.nature.com/articles/nsmb.1799 (visited on 25/05/2024).

[2] P. Arosio, T. P. J. Knowles and S. Linse, "On the lag phase in amyloid fibril formation", *Physical Chemistry Chemical Physics*, vol. 17, no. 12, pp. 7606–7618, 2015, ISSN: 1463-9076, 1463-9084. DOI: 10.1039/C4CP05563B. [Online]. Available: https://xlink.rsc.org/?DOI=C4CP05563B (visited on 26/05/2024).

[3] S. Aydin, "A short history, principles, and types of ELISA, and our laboratory experience with peptide/protein analyses using ELISA", *Peptides*, vol. 72, pp. 4–15, Oct. 2015, ISSN: 01969781. DOI: 10.1016/j.peptides.2015.04.012. [Online]. Available: https://linkinghub.elsevier.com/retrieve/pii/S019697811500131X (visited on 26/05/2024).

[4] D. D.-L. Chau, L. L.-H. Ng, Y. Zhai and K.-F. Lau, "Amyloid precursor protein and its interacting proteins in neurodevelopment", *Biochemical Society Transactions*, vol. 51, no. 4, pp. 1647–1659, 31st Aug. 2023, ISSN: 0300-5127, 1470-8752. DOI: 10.1042/BST20221527. [Online]. Available: https://portlandpress.com/biochemsoctrans/article/51/4/1647/233243/Amyloid-precursor-protein-and-its-interacting (visited on 25/05/2024).

[5] G.-f. Chen, T.-h. Xu, Y. Yan, Y.-r. Zhou, Y. Jiang, K. Melcher and H. E. Xu, "Amyloid beta: Structure, biology and structure-based therapeutic development", *Acta Pharmacologica Sinica*, vol. 38, no. 9, pp. 1205–1235, Sep. 2017, ISSN: 1671-4083, 1745-7254. DOI: 10.1038/aps.2017.28. [Online]. Available: https://www.nature.com/articles/aps201728 (visited on 13/05/2024).

[6] P. Fanjul-Bolado, M. B. González-García and A. Costa-García, "Amperometric detection in TMB/HRP-based assays", *Analytical and Bioanalytical Chemistry*, vol. 382, no. 2, pp. 297–302, May 2005, ISSN: 1618-2642, 1618-2650. DOI: 10.1007/s00216-005-3084-9. [Online]. Available: http://link.springer.com/10.1007/s00216-005-3084-9 (visited on 26/05/2024).

[7] S. Fekete, A. Beck, J.-L. Veuthey and D. Guillarme, "Theory and practice of size exclusion chromatography for the analysis of protein aggregates", *Journal of Pharmaceutical and Biomedical Analysis*, vol. 101, pp. 161–173, Dec. 2014, ISSN: 07317085. DOI: 10.1016/j.jpba.2014.04.011. [Online]. Available: https://linkinghub.elsevier.com/retrieve/pii/S0731708514002027 (visited on 25/05/2024).

[8] E. Hellstrand, B. Boland, D. M. Walsh and S. Linse, "Amyloid -protein aggregation produces highly reproducible kinetic data and occurs by a two-phase process", *ACS Chemical Neuroscience*, vol. 1, no. 1, pp. 13–18, 20th Jan. 2010, ISSN: 1948-7193, 1948-7193. DOI: 10.1021/cn900015v. [Online]. Available: https://pubs.acs.org/doi/10.1021/cn900015v (visited on 07/05/2024).

[9] S. Linse, "Expression and purification of intrinsically disordered a peptide and setup of reproducible aggregation kinetics experiment", in *Intrinsically Disordered Proteins*, B. B. Kragelund and K. Skriver, Eds., vol. 2141, Series Title: Methods in Molecular Biology, New York, NY: Springer US, 2020, pp. 731–754, ISBN: 978-1-07-160523-3 978-1-07-160524-0. DOI: 10.1007/978-1-0716-0524-0_38. [Online]. Available: https://link.springer.com/10.1007/978-1-0716-0524-0_38 (visited on 25/05/2024).

[10] S. Linse, "Toward the equilibrium and kinetics of amyloid peptide self-assembly", *Current Opinion in Structural Biology*, vol. 70, pp. 87–98, Oct. 2021, ISSN: 0959440X. DOI: 10.1016/j.sbi.2021.05.004. [Online]. Available: https://linkinghub.elsevier.com/retrieve/pii/S0959440X2100066X (visited on 26/05/2024).

[11] T. C. T. Michaels, D. Qian, A. Šarić, M. Vendruscolo, S. Linse and T. P. J. Knowles, "Amyloid formation as a protein phase transition", *Nature Reviews Physics*, vol. 5, no. 7, pp. 379–397, 27th Jun. 2023, ISSN: 2522-5820. DOI: 10.1038/s42254-023-00598-9. [Online]. Available: https://www.nature.com/articles/s42254-023-00598-9 (visited on 12/05/2024).

[12] R. Minic and I. Zivkovic, "Optimization, validation and standardization of ELISA", in *Norovirus*, G. Mózsik, Ed., IntechOpen, 1st Sep. 2021, ISBN: 978-1-83968-944-4 978-1-83968-945-1. DOI: 10.5772/intechopen.94338. [Online]. Available: https://www.intechopen.com/books/norovirus/optimization-validation-and-standardization-of-elisa (visited on 20/05/2024).

[13] J. Simrén, A. Elmgren, K. Blennow and H. Zetterberg, "Fluid biomarkers in alzheimer's disease", in *Advances in Clinical Chemistry*, vol. 112, Elsevier, 2023, pp. 249–281, ISBN: 978-0-443-19284-5. DOI: 10.1016/bs.acc.2022.09.006. [Online]. Available: https://linkinghub.elsevier.com/retrieve/pii/S0065242322000749 (visited on 25/05/2024).

[14] S. Subedi, S. Sasidharan, N. Nag, P. Saudagar and T. Tripathi, "Amyloid cross-seeding: Mechanism, implication, and inhibition", *Molecules*, vol. 27, no. 6, p. 1776, 8th Mar. 2022, ISSN: 1420-3049. DOI: 10.3390/molecules27061776. [Online]. Available: https://www.mdpi.com/1420-3049/27/6/1776 (visited on 26/05/2024).

[15] K. Y. Wu, D. Doan, M. Medrano and C.-e. A. Chang, "Modeling structural interconversion in alzheimers' amyloid beta peptide with classical and intrinsically disordered protein force fields", *Journal of Biomolecular Structure and Dynamics*, vol. 40, no. 20, pp. 10 005–10 022, 29th Nov. 2022, ISSN: 0739-1102, 1538-0254. DOI: 10.1080/07391102.2021.1939163. [Online]. Available: https://www.tandfonline.com/doi/full/10.1080/07391102.2021.1939163 (visited on 26/05/2024).